Higher levels of advanced glycation endproducts in human carotid atherosclerotic plaques are associated with a rupture-prone phenotype

European Heart Journal (2014) **35**, 1137–1146
doi:10.1093/eurheartj/eht402

Higher levels of advanced glycation endproducts in human carotid atherosclerotic plaques are associated with a rupture-prone phenotype

Nordin M.J. Hanssen[1,2], Kristiaan Wouters[1,2], Maya S. Huijberts[1,2], Marion J. Gijbels[1,3,4,5], Judith C. Sluimer[1,5], Jean L.J.M. Scheijen[1], Sylvia Heeneman[1,5], Erik A.L. Biessen[1,5], Mat J.A.P. Daemen[1,6], Michael Brownlee[7], Dominique P. de Kleijn[8,9], Coen D.A. Stehouwer[1,2], Gerard Pasterkamp[8], and Casper G. Schalkwijk[1,2]*

[1]Cardiovascular Research Institute Maastricht (CARIM), Maastricht University Medical Centre (MUMC), Maastricht, The Netherlands; [2]Department of Internal Medicine, Laboratory for Metabolism and Vascular Medicine, MUMC, Debeyelaan 25, PO Box 5800, Maastricht, AZ 6202, The Netherlands; [3]Department of Molecular Genetics, MUMC, Maastricht, The Netherlands; [4]Department of Medical Biochemistry, Amsterdam Medical Centre, Amsterdam, The Netherlands; [5]Department of Pathology, MUMC, Maastricht, The Netherlands; [6]Department of Pathology, Amsterdam Medical Centre, Amsterdam, The Netherlands; [7]Albert Einstein Diabetes Research Center, Albert Einstein College of Medicine, New York, NY, USA; [8]Laboratory of Experimental Cardiology and ICIN, UMC Utrecht, The Netherlands; and [9]Surgery and CVRI, NUS, Singapore

Received 11 January 2013; revised 16 August 2013; accepted 11 September 2013; online publish-ahead-of-print 14 October 2013

See page 1095 for the editorial comment on this article (doi:10.1093/eurheartj/eht454)

Aims Rupture-prone atherosclerotic plaques are characterized by inflammation and a large necrotic core. Inflammation is linked to high metabolic activity. Advanced glycation endproducts (AGEs) and their major precursor methylglyoxal are formed during high metabolic activity and can have detrimental effects on cellular function and may induce cell death. Therefore, we investigated whether plaque AGEs are increased in human carotid rupture-prone plaques and are associated with plaque inflammation and necrotic core formation.

Methods and results The protein-bound major methylglyoxal-derived AGE 5-hydro-5-methylimidazolone (MG-H1) and N^{ε}-(carboxymethyl)lysine (CML) were measured in human carotid endarterectomy specimens ($n = 75$) with tandem mass spectrometry. MG-H1 and CML levels were associated with rupture-prone plaques, increased protein levels of the inflammatory mediators IL-8 and MCP-1 and with higher MMP-9 activity. Immunohistochemistry showed that AGEs accumulated predominantly in macrophages surrounding the necrotic core and co-localized with cleaved caspase-3. Intra-plaque comparison revealed that glyoxalase-1 (GLO-1), the major methylglyoxal-detoxifying enzyme, mRNA was decreased (-13%, $P < 0.05$) in ruptured compared with stable plaque segments. In line, in U937 monocytes, we found reduced (GLO-1) activity (-38%, $P < 0.05$) and increased MGO (346%, $P < 0.05$) production after stimulation with the inflammatory mediator TNF. Direct incubation with methylglyoxal increased apoptosis up to two-fold.

Conclusion This is the first study showing that AGEs are associated with human rupture-prone plaques. Furthermore, this study suggests a cascade linking inflammation, reduced GLO-1, methylglyoxal- and AGE-accumulation, and subsequent apoptosis. Thereby, AGEs may act as mediators of the progression of stable to rupture-prone plaques, opening a window towards novel treatments and biomarkers to treat cardiovascular diseases.

Keywords Atherosclerosis • Advanced glycation endproducts • Cell death • Glyoxalase • Macrophage • Plaque rupture

Introduction

Rupture of an atherosclerotic plaque and subsequent thrombosis is the major cause of cardiovascular events such as heart attack and stroke.[1,2] The major histological components of rupture-prone plaques are inflammation, macrophage infiltration, and a large necrotic core.[3]

Inflammation of the plaque is characterized by high metabolic activity in macrophages, as characterized by high ^{18}Fluor-deoxyglucose

* Corresponding author. Tel: +31 43 3882186, Fax: +31 43 3875006, Email: c.schalkwijk@maastrichtuniversity.nl

uptake,[4] hypoxia,[5] and oxidative stress.[6] Advanced glycation endproducts (AGEs) are a large family of extensively sugar-modified proteins which can be formed in plaques as a consequence of increased metabolic activity.[7] Indeed, we and others have demonstrated that AGEs, including major AGE N^{ε}-(carboxymethyl)lysine (CML), are present in atherosclerotic lesions.[8–11] Moreover, animal studies have shown that therapies decreasing AGEs attenuate atherosclerosis.[12–14] Despite the clear link between AGEs and atherosclerosis, their precise mechanism of action remains largely unknown.

It is becoming apparent that especially intracellular sugars and their derivatives can induce AGE formation, with the dicarbonyl methylglyoxal (MGO) as the most reactive AGE precursor.[15] MGO reacts primarily with arginine residues to form the non-fluorescent AGE 5-hydro-5-methylimidazolone (MG-H1). MGO-derived AGEs have been linked to vascular complications,[16] generation of free oxygen radicals,[17] and apoptosis.[18,19] MGO can be detoxified by glyoxalase 1 (GLO-1), GLO-2 and reduced glutathione[20] into D-lactate, thereby preventing accumulation of MGO and MGO-derived AGEs. Therefore, we hypothesized that reduced GLO-1 activity, production of MGO, and subsequent AGEs may be a major factor contributing to the association between plaque inflammation and necrotic core formation, which in turn may predispose plaques to rupture.

In rupture-prone plaques, i.e. plaques with an inflammatory atheromatous phenotype, we found higher plaque AGEs, which accumulated in macrophages, and co-localized with cleaved caspase-3 and hypoxia. Moreover, GLO-1 was decreased in ruptured plaques. In line, we showed a direct role of MGO on apoptosis *in vitro*. Taken together, our data suggest that decreased GLO-1 and increased MGO and AGEs arise in metabolically active plaques, and may contribute to plaque rupture by inducing apoptosis of macrophages, increasing the size of the necrotic core.

Methods

An elaborate description of the Methods is provided in the Supplementary material online.

Athero-express biobank

This study included a random set of 75 plaques from symptomatic ($n = 62$) and asymptomatic ($n = 13$) patients undergoing carotid endarterectomy (CEA) from the Athero-Express biobank. The study was approved by the local Ethics Committee and written informed consent was obtained from all participants. Plaques of the inflammatory and atheromatous phenotype, i.e. high macrophages and lipid scores, and with low smooth muscle cell scores were classified as rupture-prone ($n = 20$). Plaques with a fibrous phenotype, low macrophage, and lipid scores, and high smooth muscle cell content were characterized as stable ($n = 26$). Plaques not falling in either category were classified as intermediate plaques ($n = 29$).

Measurement of advanced glycation endproducts using tandem mass spectrometry

Protein-bound CML, and MGO-derived AGEs N^{ε}-(carboxyethyl)lysine (CEL) and MG-H1 were measured in homogenates of carotid plaques using ultra performance liquid chromatography tandem mass spectrometry (UPLC-MSMS) by a slightly modified single-run method described earlier.[21] Intra-assay variation for CML, CEL, and MG-H1 was 4.8, 5.0, and 18.1%, respectively. All samples of the Athero-Express were measured in a single run, eliminating inter-run variation.

Protein measurements

Plaque cytokines and chemokines (*Table 2*) were measured by a multiplex suspension array system according to the manufacturer's protocol (Bender Med Systems). Matrix metalloprotease (MMP)-2, MMP-8, and MMP-9 activities were measured using the Biotrak activity assays (Amersham Biosciences).

IL-8, MCP-1, and MMP-9 in cell-culture supernatant were measured using Meso Scale Discovery (Gaithersburg, USA) multispot human cytokine assays for tissue cultures according to manufacturer's instructions.

Immunohistochemistry

A random set of 40 plaques from the Athero-Express was selected for immuno-histological analysis. Consecutive sections were stained with a mouse monoclonal antibody anti-MG-H1 (1:50.000) and anti-CML (1:4000).[11] Horseradish peroxidase-antimouse IgG (Immunologic) was used as a secondary antibody.

In addition, stainings were performed with anti-CD68 (1:500, Sigma), GLO-1 (1:2000), and cleaved caspase-3 (1:100, Cell signaling) on carotid plaques, obtained from CEA, from the biobank of the Cardiovascular Research Institute of Maastricht (CARIM), Maastricht University.

Staining for hypoxia (mouse anti-pimonidazole 1:50, hypoxyprobe, NPI)) and oxidative stress (mouse anti-nitrotyrosine 1:500, Calbiochem, San Diego, USA) were performed on slides of carotid arteries obtained from 13 patients, infused with pimonidazole prior to CEA.[5]

CARIM biobank (transcript and protein analysis of GLO-1 and RAGE)

An intra-plaque comparison approach consisting of CEA atherosclerotic plaque samples that were selected from the CARIM biobank at Maastricht University, the Netherlands, for transcript and protein analysis was used to compare GLO-1 and RAGE mRNA and protein between ruptured and stable plaque segments ($n = 26$).

GLO-I activity was assayed by spectrophotometry (Synergy, Biotek) by monitoring the increase in absorbance at 240 nm due to the formation of *S*-D-lactoylglutathione for 10 min at 37°C according to the method of McLellan and Thornalley,[22] in homogenates of stable plaques ($n = 4$) and plaques with an intra-plaque haemorrhage ($n = 6$).

In vitro experiments

Human U937 monocytes (ATCC) were cultured in RPMI 1640 with glutamax (GIBCO), with 1% penicillin and streptomycin (GIBCO) and 10% foetal calf serum. Cells were cultured for 24 h in 0% oxygen and 48 h in 0.2% oxygen. To study hyperglycaemia, cells were cultured for 14 days in high glucose (30 mmol/L), or mannitol, as an osmotic control.

Cells were stimulated in serum-free culture medium with 0.2% bovine serum albumin, and exposed for 24 h to tumour necrosis factor (TNF, Sigma) (100 U/mL), aminoguanidine (Sigma) (250μmol/l), *N*-acetylcysteine (NAC, Sigma) (1 mmol/L), H_2O_2 (1 or 10 μmol/L), and/or to MGO (Sigma) (0.1 mmol/L, 0.2 and 0.4 mmol/L). Next, U937 monocytes were exposed for 24 h to human serum albumin (HSA, 33 μg/mL) and CML-modified HSA. U937 monocytes were transfected with siRNA against GLO-1 (Ambion) with AMAXA nucleofector kit C (Lonza) by electroporation, according to the manufacturer's protocol. Apoptosis was assessed by flow cytometry (FACS) using annexin-V and 7-AAD following the manufacturer's instructions (BD Pharmingen). Cell viability was assessed by an 3-(4,5-dimethylthiazol-2-yl)-2,5-diphenyl tetrazolium bromide (MTT; Invitrogen) assay. GLO-1 mRNA expression was assayed

by qPCR. CML and MG-H1 were quantified in cell lysate with western blot. β-Actin was used as a loading control.

Murine macrophages

Bone marrow-derived murine macrophages were obtained by differentiating femoral and tibial bone marrow suspensions as described previously.[23] Bone marrow was isolated from 10-week-old C57BL6 mice (JAX® Mice). Experiments were performed according to Dutch laws, approved by the Committee for Animal Welfare of Maastricht University. At Day 9, the macrophages were plated in OptiMEM (GIBCO) and incubated with or without mouse TNF (Peprotech, 500 U/mL) and MGO (0.1 mmol, 0.2 mmol/L, and 0.4 mmol/L) for 24 h. Cell death (SubG1 peak) and proliferation (S and G2M peak) was assessed by FACS using Propidium–Iodine, following the manufacturer's instructions (BD cycletest).

MGO and glyoxal

Secretion of MGO, as well as glyoxal (GO) in culture medium were measured with UPLC-MSMS.[24] Inter-assay variations for MGO and GO were 7.3 and 14.3%, respectively. Intra-assay variations for MGO and GO were 2.9 and 4.3% respectively.

Data analysis

Patient characteristics were expressed as absolute and relative frequencies, as mean with standard deviation, or as median with interquartile range, when appropriate. Increases in patient characteristics per plaque category were tested for trend, using analysis of variance (ANOVA) or χ^2, as appropriate. Next, associations between plaque AGE levels and categories of plaque phenotype and inflammatory markers were assessed with analysis of co-variance (ANCOVA) and linear regression, respectively, adjusting for sex, age, smoking, and presence of diabetes, to rule out potential confounding by these factors. Skewed variables were log-transformed prior to all analyses. Results from *in vitro* experiments were presented as mean with standard error, and statistical significance of the difference between two groups was tested by Student's

Table 1 General characteristics of individuals, stratified according to plaque phenotype, from the Athero-Express study ($n = 75$)

Patient characteristics	Plaque phenotype			
	Stable ($n = 26$)	Intermediary ($n = 29$)	Rupture-prone ($n = 20$)	*P*-value
Age, years	67 ± 9	68 ± 9	69 ± 8	0.44
Sex (male), %	69.2	72.4	75.0	0.67
Smoking, %	26.9	37.0	15.8	0.49
Systolic blood pressure, mmHg	160 ± 24	150 ± 32	160 ± 25	0.97
Diastolic blood pressure, mmHg	83 ± 15	81 ± 13	85 ± 14	0.67
History of hypertension, %	73.1	75.9	55.0	0.22
eGFR, mL/min/1.73 m^2	71.6 ± 20.8	70.4 ± 25.6	64.1 ± 16.8	0.25
C-reactive protein, mg/L	2.1 (0.9–4.5)	6.1 (3.0–11.4)	5.2 (0.6–6.4)	0.59
Plasma glucose, mmol/L	6.4 ± 2.1	6.5 ± 2.6	7.7 ± 2.21	0.15
History of diabetes, %	53.8	51.7	50.0	0.80
Insulin use, %	23.1	24.1	15.0	0.54
Glucose-lowering medication, %	42.3%	37.1%	45%	0.89
Body mass index, kg/m^2	26.3 ± 3.2	28.2 ± 4.9	27.4 ± 4.2	0.39
History of hypercholesterolaemia, %	73.1	89.7	50.0	0.13
Total cholesterol, mmol/L	4.4 ± 0.9	5.1 ± 1.9	4.7 ± 1.0	0.71
High-density lipoprotein, mmol/L	1.2 ± 0.4	1.2 ± 0.3	1.2 ± 0.4	0.88
Low-density lipoprotein, mmol/L	2.4 ± 0.7	3.2 ± 1.7	2.8 ± 0.7	0.53
Triglycerides, mmol/L	1.9 (0.9–2.6)	1.3 (1.1–2.3)	1.4 (1.0–2.1)	0.44
Statin use, %	92.3	82.8	80.0	0.23
Transient ischaemic attack, %	26.9	34.5	50.0	0.11
Minor stroke, %	15.4	24.1	10.0	0.68
Stroke, %	3.8	6.9	5.0	0.84
Amaurosis fugax, %	26.9	20.7	5.0	0.06
Retinal infarction, %	0	0	5.0	0.16
Atypical symptoms, %	3.8	3.4	5.0	0.86
Plaque AGEs				
CML, nmol/mmol lysine	70.85 (58.78–88.92)	92.30 (65.55–140.05)	126.35 (62.40–211.08)	**<0.02**
CEL, nmol/mmol lysine	90.50 (79.98–103.15)	91.00 (73.20–110.0)	98.50 (87.40–109.38)	0.15
MG-H1, nmol/mmol lysine	320.35 (272.72–431.30)	392.00 (297.95–841.50)	524.70 (346.35–965.70)	**<0.01**

Data expressed as mean ± standard deviation, as percentage, or as median and interquartile range, as appropriate. Statistical testing was performed for trend, using one-way ANOVA, or χ^2 test, as appropriate. Skewed variables were log-transformed prior to analyses.
AGE, advanced glycation endproduct.

t-test for two independent samples. Probability values < 0.05 were considered significant.

Results

CML and methylglyoxal-derived AGE MG-H1 plaque levels are higher in rupture-prone plaques

We first investigated whether plaque MGO-derived AGE levels are associated with a rupture-prone phenotype in human carotid plaques. The clinical characteristics of the included patients are shown in *Table 1*.

Significantly higher concentrations of CML and MG-H1, but not CEL, were observed in rupture-prone plaques (*Table 1*), even after adjustment for sex, age, smoking, and presence of diabetes (*Figure 1*). Additionally, higher MG-H1 concentrations were observed with increasing percentage of plaque lipid content (Supplementary material online, *Figure S1A*), and a similar trend was observed for CML (Supplementary material online, *Figure S1B*). In line, higher MG-H1 levels were observed in atheromatous lesions compared with fibrous lesion types (Supplementary material online, *Figure S1A*). Interestingly, no increase of plaque AGEs were observed in patients with diabetes ($n = 39$) when compared with non-diabetic patients ($n = 36$) for CML [79.0 (58.6–126.3) vs. 90.6 (65.6–150.1) nmol/mmol lysine, $P = 0.23$], CEL [89.2 (82.0–106.9) vs. 93.4 (75.7–109.0) nmol/mmol lysine,

Table 2 Associations between plaque advanced glycation endproducts and plaque interleukins and matrix metalloproteinases

	CML			CEL			MG-H1		
	β	95% CI for β	*P*-value	β	95% CI for β	*P*-value	β	95% CI for β	*P*-value
IL-8	0.307	0.077–0.537	<0.05	0.118	−0.128–0.364	0.34	0.295	0.047–0.544	<0.05
MCP-1	0.240	−0.27–0.506	0.08	0.275	0.001–0.548	<0.05	0.314	0.041–0.588	<0.05
MMP-9	0.421	0.196–0.647	<0.05	0.290	0.052–0.528	<0.05	0.409	0.173–0.646	<0.05
IL-6	0.142	−0.105–0.388	0.26	−0.021	−0.275–0.234	0.87	0.158	−0.105–0.421	0.24
RANTES	0.088	−0.222–0.397	0.57	0.314	−0.011–0.638	0.06	0.230	−0.104–0.564	0.17
PARC	−0.023	−0.289–0.224	0.80	0.178	−0.084–0.440	0.18	0.114	−0.152–0.380	0.39
TARC	−0.079	−0.341–0.182	0.55	0.057	−0.213–0.328	0.67	0.025	−0.249–0.298	0.18
OPG	−0.045	−0.644–0.553	0.88	0.711	0.118–1.305	<0.05	0.319	−0.300–0.938	0.31
sICAM	−0.029	−0.291–0.232	0.82	0.042	−0.227–0.311	0.76	−0.032	−0.305–0.241	0.82
MMP-2	−0.014	−0.272–0.244	0.91	0.254	0.003–0.506	<0.05	0.117	−0.148–0.383	0.38
MMP-8	0.157	−0.089–0.403	0.21	0.223	−0.020–0.466	0.07	0.198	−0.055–0.451	0.12

The table shows associations between plaque levels of CML, CEL, and MG-H1 with IL-8: interleukin 8, MCP-1, monocyte chemotactic protein-1; MMP-9, matrix metalloproteinase-9; IL-6, interleukin 6; RANTES, regulated on activation, normal t expressed and secreted; PARC, pulmonary and activation-regulated chemokine; TARC, thymus and activation-regulated chemokine; OPG, osteoprotegerin; sICAM, soluble inter-cellular adhesion molecule; MMP-2, matrix metalloproteinase-2; MMP-8, matrix metalloproteinase-8.
Data were analysed using linear regression, all skewed variables were log-transformed prior to analysis and adjusted for age, sex, smoking, and presence of diabetes. The plaque AGEs were the dependent variable. *β* indicates 1 standard deviation increase of log-transformed AGE per 1 standard deviation increase log-transformed inflammatory marker.

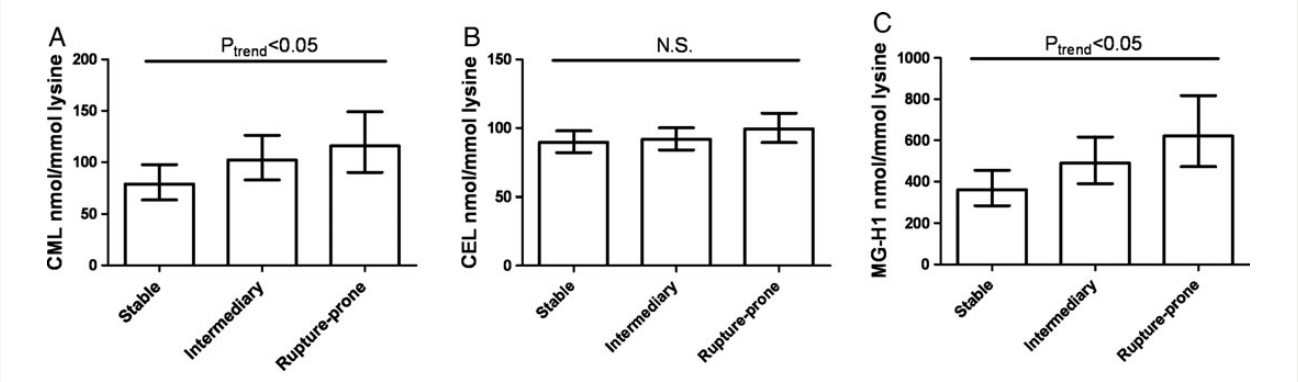

Figure 1 CML and MG-H1 levels are higher in plaques with an intermediary and rupture prone phenotype. Concentrations of CML (*A*), CEL (*B*), and MG-H1 (*C*) were measured with UPLC-MSMS in homogenates of atherosclerotic carotid plaques from the Athero-Express study with a stable, intermediary, and rupture-prone phenotype. Data are expressed as geometric mean and 95% confidence interval. Statistical testing was performed for trend, using ANCOVA. Skewed variables were log-transformed. Analyses were adjusted for age, sex, smoking, and the presence of diabetes.

$P = 0.97$], and MG-H1 [367.0 (307.0–866.7) vs. 406.2 (288.2–660.0) nmol/mmol lysine, $P = 0.95$]. In line, we also found no correlation between plaque levels of CML ($\rho_{Spearman} = -0.118$, $P = 0.40$), CEL ($\rho_{Spearman} = -0.238$, $P = 0.09$), and MG-H1 ($\rho_{Spearman} = -0.129$, $P = 0.36$) with plasma glucose levels. These results did not change when we adjusted for insulin-use and/or glucose-lowering medication in a linear regression analyses.

CML, CEL, and methylglyoxal-derived AGE MG-H1 plaque levels are associated with markers of plaque inflammation

Since AGEs accumulate in the areas of inflammatory activation in atherosclerotic lesions,[25] we investigated the associations between plaque AGE levels and plaque inflammatory markers. CML, CEL, and MG-H1 were positively associated with MMP-9 (*Table 2*). Furthermore, CEL and MG-H1 were positively associated with MCP-1 (*Table 2*), and this was borderline significant for CML. In addition, CML and MG-H1 were associated with IL-8 (*Table 2*). Furthermore, CEL was associated with OPG and MMP-2 (*Table 2*).

CML and methylglyoxal-derived AGE MG-H1 accumulate in apoptotic and hypoxic macrophages

Staining for CML and MG-H1 was observed predominantly in macrophages (*Figure 2*, CD68 positive cells; black arrows) surrounding the necrotic core (*Figure 2*, asterisk). In addition, these macrophages were also positive for the apoptotic marker cleaved caspase-3 (*Figures 2* and *3*), suggesting that MGO-derived AGEs play a role in the association between plaque inflammation and necrotic core formation. Furthermore, in consecutive sections, MG-H1 and CML also co-localized with hypoxia (pimonidazole) (*Figure 3*), which is particularly associated with the presence of macrophages, inflammation, and apoptosis. We also observed co-localization between CML, MG-H1, and the oxidative stress marker nitrotyrosine (Supplementary material online, *Figure S2*), but unlike caspase-3 and pimonidazole, we also encountered areas where only nitrotyrosine, but not CML or MG-H1, was accumulated. In addition to macrophages, endothelial cells often stained positive for CML (*Figures 2* and *3*, white arrows) and for MG-H1 (*Figures 2* and *3*, white arrows).

Glyoxalase-1 mRNA and protein level, but not receptor for advanced glycation endproducts mRNA, are lower in ruptured plaque areas

Underlining the importance of GLO-1 in maintaining cell-viability, GLO-1 staining was abundantly present in the cytoplasm of virtually all cells of the plaque (*Figure 2*), but not in the necrotic core. Moreover, micro-array data demonstrated that GLO-1 mRNA was significantly lower in ruptured plaque-segments when compared with stable plaque-segments (ratio ruptured/stable = 0.874; $P < 0.01$). In addition, GLO-1 protein levels were decreased to a similar extent in ruptured compared with stable segments (ratio ruptured/stable = 0.871), although this was not statistically significant. The same was true when we measured GLO-1 activity in homogenates of stable and ruptured plaques (ratio ruptured/stable = 0.613). In contrast to GLO-1, we found no differences in RAGE expression between stable and ruptured plaque segments (ratio ruptured/stable = 0.994; $P = 0.53$)

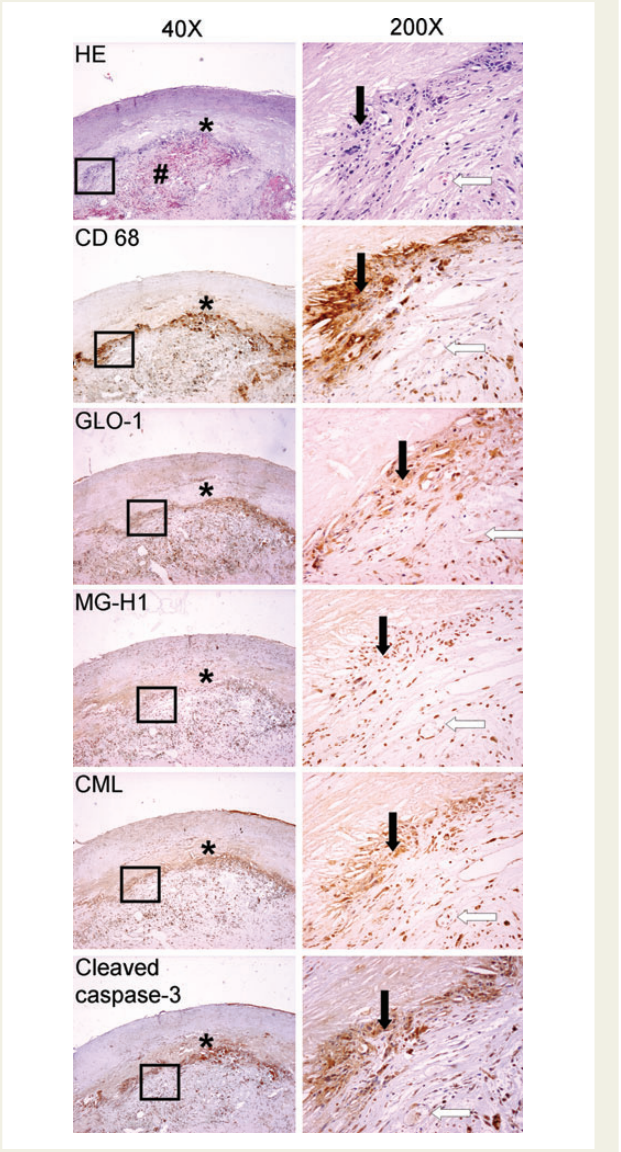

Figure 2 CML and MG-H1 co-localization with macrophages (CD68), and apoptosis (cleaved caspase-3). HE stainings and immunohistochemical detection of CD 68, GLO-1, CML, MG-H1, and cleaved caspase-3 were performed in CEA specimens. The HE-staining shows an extensive macrophage infiltration surrounding a large intra-plaque haemorrhage (hashtag) in the necrotic core (asterisk). CML and MG-H1 accumulated predominantly in macrophages (CD68), especially in apopototic macrophages (cleaved caspase-3) surrounding the necrotic core. Black arrows indicate macrophages, white arrows indicate plaque vessels. The square indicates zoomed areas.

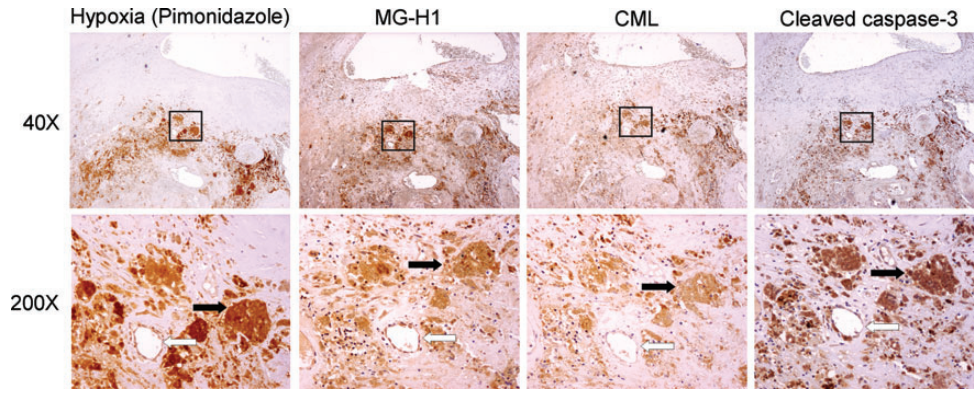

Figure 3 CML and MG-H1 co-localize with hypoxic regions. Plaques of patients infused with hypoxia marker pimonidazole were stained for pimonidazole, cleaved caspase-3, CML, and MG-H1. We observed a striking co-localization between hypoxia (pimonidazole), CML, MG-H1, and apoptosis (cleaved caspase-3). Black arrows indicate macrophages, white arrows indicate plaque vessels. The square indicates zoomed area.

Hypoxia and tumour necrosis factor decrease glyoxalase I activity and increase advanced glycation endproduct precursors

Since CML and MG-H1 co-localized with macrophage-rich and hypoxic regions, and we found decreased GLO-1 expression and activity in ruptured plaques, we investigated in U937 monocytes whether hypoxia and inflammation can decrease GLO-1 activity and induce formation of the major AGE precursors (in particular MGO).

We first investigated whether hypoxia contributed to accumulation of AGEs. U937 monocytes cultured in 0.2% O_2 induced a reduction of GLO-1 activity (*Figure 4A*) and increased MGO (*Figure 4B*) and GO (*Figure 4C*) levels. This effect was much stronger when the cells were cultured in 0% O_2 (Supplementary material online, *Figure S3*).

Next, activation of cells with the pro-inflammatory cytokine TNF decreased GLO-1 activity (*Figure 4D*), accompanied by increased formation of MGO (*Figure 4E*), and the AGEs MG-H1 (*Figure 4G* and *H*) and CML (*Figure 4I* and *J*), as well as IL-8 (*Figure 4K*), MCP-1 (*Figure 4L*), and MMP-9 (*Figure 4M*). Similarly, GLO-1 activity was also reduced (Supplementary material online, *Figure S4A*), and MGO increased (Supplementary material online, *Figure S4B*), when we stimulated murine macrophages with TNF.

The TNF-induced accumulation of AGEs in U937 monocytes was not dependent on oxidative stress, as co-incubation with NAC did not restore GLO-1 activity or reduce MGO or CML (Supplementary material online, *Figure S5*). However, incubation of U937 monocytes with H_2O_2 strongly increased CML (Supplementary material online, *Figure S6*), suggesting that high levels of oxidative stress may act as an independent source of AGEs. In line with the Athero-Express, high glucose did not significantly influence GLO-1 activity, MGO, or AGE levels in U937 monocytes (Supplementary material online, *Figure S7*).

The inflammatory response of TNF on IL-8, MCP-1, or MMP-9 was not dependent on AGEs, because the AGE-inhibitor aminoguanidine lowered MGO and AGEs (data not shown) but did not decrease IL-8 (*Figure 4K*), MCP-1 (*Figure 4L*), or MMP-9 (*Figure 4M*) secretion. In line, direct incubation of monocytes with CML or MGO did not increase the secretion of IL-8 (*Figure 4K*), MCP-1 (*Figure 4L*), or MMP-9 (*Figure 4M*).

Methylglyoxal induces apoptosis

Since MG-H1 and CML predominantly accumulated in apoptotic macrophages around the necrotic core, and major AGE precursor MGO is associated with inducing apoptosis,[18,19] we investigated the effect of MGO on U937 cell-viability. MGO induced formation of MG-H1(Supplementary material online, *Figure S8A* and *B*), and to a lesser extent CML (Supplementary material online, *Figure S8C* and *D*) as well as a dose-dependent increase in AAD-7 and Annexin-V double positive cells, indicating apoptotic cells (*Figure 5A–C*). In line, MGO induced cell-death in murine macrophages (Supplementary material online, *Figure S4F*), but did not decrease proliferation, as assayed with propidium–iodine (S-peak and G2/M peak) (Supplementary material online, *Figure S4G* and *H*).

We next investigated whether decreased GLO-1, as found in the ruptured plaque-segments, reduced cell-viability of U937 monocytes. In untreated cells, siRNA against GLO-1 lowered GLO-1 activity (*Figure 5D*) and mRNA expression (*Figure 5E*), but did not increase endogenous MGO production (*Figure 5F*) and cell viability (*Figure 5G*). However, when challenged with MGO, the transfected cells displayed decreased MGO-induced cell viability compared with the scrambled-treated cells (*Figure 5H* and *I*), demonstrating that GLO-1 is important to protect cells from the cytotoxic effects of MGO.

Discussion

Our study shows for the first time that the plaque concentrations of the specific AGEs CML and MG-H1 are associated with inflammatory plaque markers and were higher in rupture-prone plaques (i.e. inflammatory atheromatous lesions). CML and MG-H1 predominantly localized in macrophages surrounding the necrotic core, and were associated with apoptosis and hypoxia. In ruptured plaque segments, GLO-1 mRNA and protein concentrations were reduced. In U937 monocytes, TNF and hypoxia decreased GLO-1 activity and

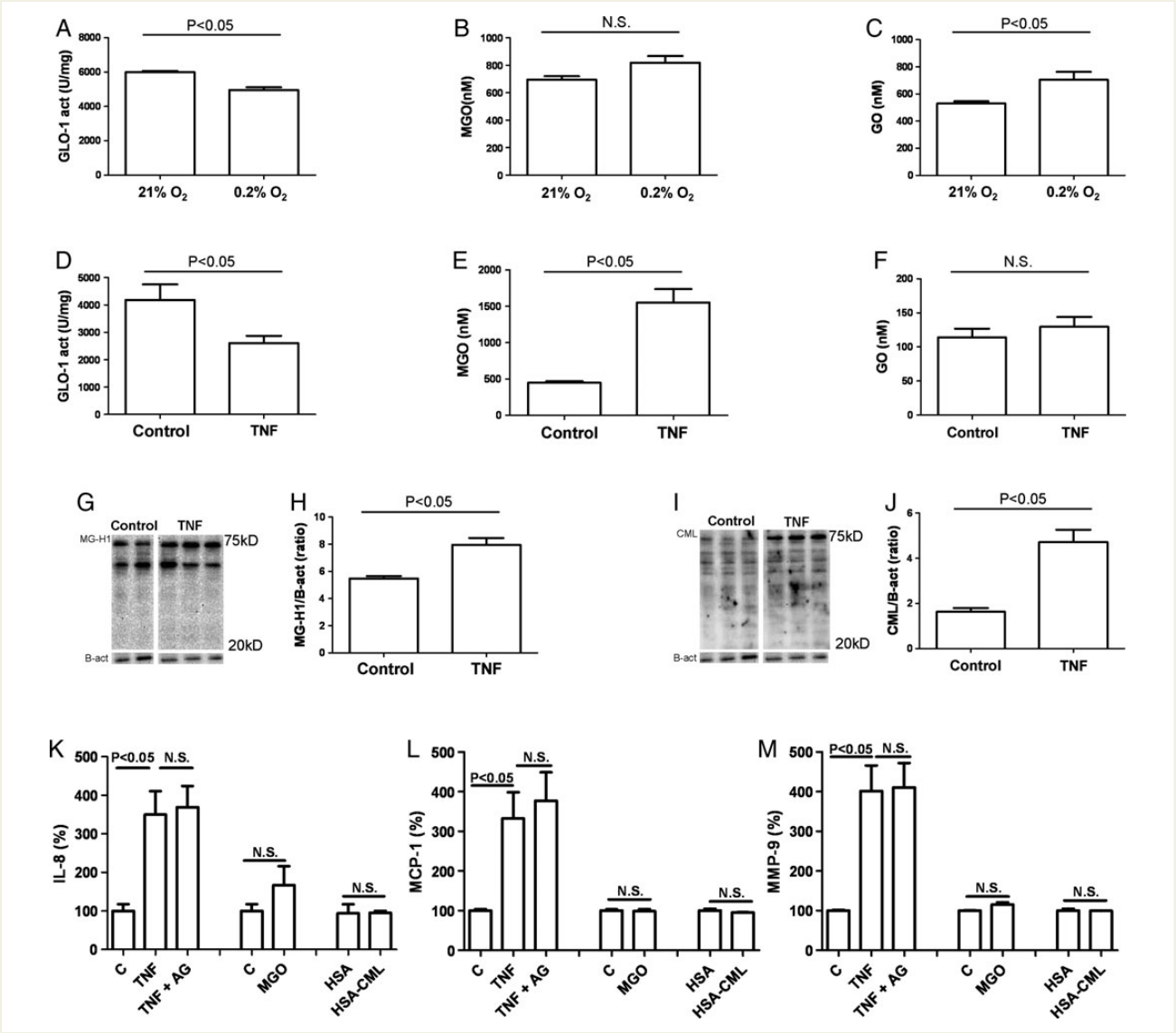

Figure 4 Hypoxia and tumour necrosis factor inhibit GLO-1 activity and induce MGO in U937 monocytes. U937 cells were cultured under hypoxic conditions (0.2% O_2) for 48 h or with tumour necrosis factor (100 U/mL) for 24 h. GLO-1 activity (*A* and *D*) was measured. MGO (*B* and *E*) and GO (*C* and *F*) were measured in the culture supernatant with UPLC-MSMS. MG-H1 (*G*, quantification *H*) and CML (*I*, quantification *J*) were measured with western-blot in the cell-lysate. β-actin was used as a loading control. U937 monocytes were treated with tumour necrosis factor, aminoguanidine (AG), MGO, and HSA-CML, and protein levels of IL-8 (*K*), MCP-1 (*L*), and MMP-9 (*M*) were measured in the supernatant. Data are presented as mean and standard error. Differences were tested with Student's *t*-test for two independent samples.

increased the production of the AGE precursor MGO. MGO induced AGE formation and caused apoptosis, which was enhanced by GLO-1 knock-down, providing functional evidence for the involvement of GLO-1 in MGO-mediated apoptosis. Taken together, these results suggest that the increase of AGEs and consequences thereof for macrophage cell death may contribute to the transition of stable to rupture-prone plaques.

To our knowledge, this is the first study in which specific AGEs were quantified in homogenates of atherosclerotic plaques using UPLC-MSMS. Several studies have shown with immunohistochemistry that AGEs accumulate in atherosclerotic lesions of the aorta,[8,26,27] coronary[9] and carotid arteries using antibodies against CML or glycation-modified proteins. In accordance with previous studies,[25,26,28,29] we identified the macrophage as the major site for AGE accumulation in the plaque.

Advanced glycation endproducts can be derived from several pathways in atherosclerotic lesions. Previous work from our group has demonstrated the importance GLO-1 as a critical defense line against glycation *in vivo*.[30] We hypothesized that inflammation and hypoxia in atherosclerotic plaques contribute to increased concentrations of AGEs by decreased GLO-1 expression. Indeed, in U937 monocytes TNF, a strong pro-inflammatory stimulus, as well as hypoxia, decreased GLO-1 activity, accompanied by increased MGO production. Importantly, we found similar effects of TNF on

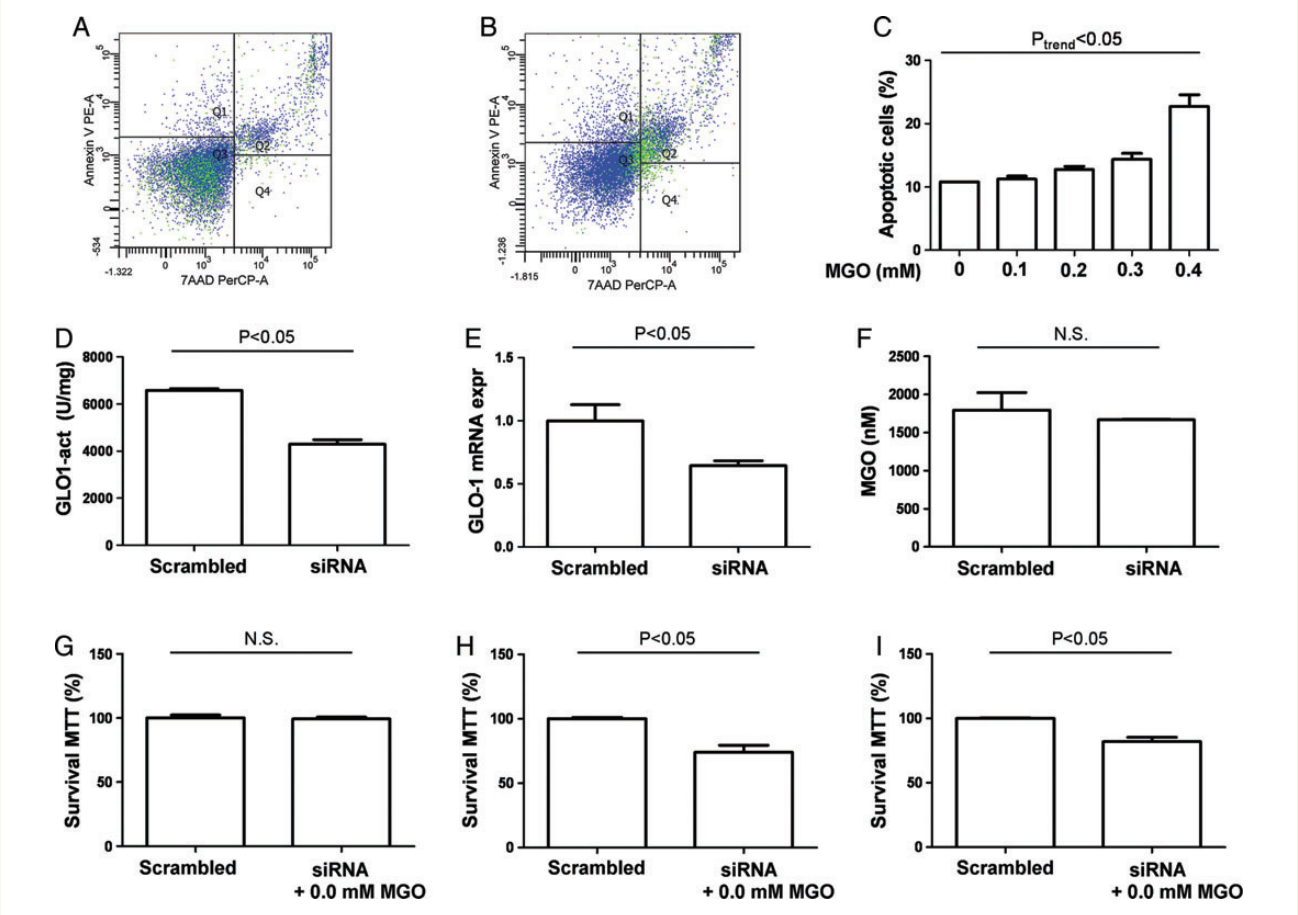

Figure 5 GLO-1 knockdown reduces viability after incubation with MGO in U937 monocytes. U937 cells were incubated for 24 h with 0.1, 0.2, 0.3, and 0.4 mM MGO, and apoptosis was assessed by flowcytometric analyses for Annexin-V and 7-AAD (*A*, control; *B*, 0.4 mmol/L MGO, quantification in *C*). Statistical testing was performed for trend, using ANOVA. Next, U937 cells were transfected with siRNA against GLO-1, and GLO-1 activity (*D*) and mRNA (*E*) were measured. MGO (*F*) was measured with UPLC-MSMS in the culture supernatant. Next, cells were incubated with MGO for 24 h and viability was measured by an MTT assay (*G*, 0 mmol/L MGO; *H*, 0.2 mmol/L MGO; and *I*, 0.4 mmol/L MGO). Data are presented as mean and standard error. Differences were tested with Student's *t*-test for two independent samples.

GLO-1 and MGO in murine macrophages. In line with a previous report,[31] high glucose did not materially contribute to accumulation of AGEs in U937 monocytes.

One of the hallmarks of rupture-prone plaques is a large necrotic core. In human carotid plaques, CML and MG-H1 were predominantly present in caspase-3 positive macrophages surrounding necrotic regions of the plaque. Furthermore, MGO induced cell-death in monocytes and murine macrophages, a finding which is consistent with previously reported data.[18,19] We hypothesize that this may lead to a vicious cycle of inflammation, increased formation of MGO (and AGEs), inducing apoptosis of macrophages, growth of necrotic core, up to the point that plaque rupture occurs. This process may be aggravated by hypoxia and oxidative stress. We showed the importance of GLO-1 in protecting cells against toxic effects of MGO by showing decreased viability of U937 monocytes after GLO-1 knockdown. Therefore, our current work suggests that GLO-1 may protect against plaque rupture. To support this notion, we found decreased expression of GLO-1 in ruptured vs. stable plaque segments. We hypothesize that interventions aimed at restoring the glyoxalase pathway and/or reducing MGO levels in the plaque, will reduce glycation, and subsequently will reduce cell-death and necrotic core size. Future studies are needed to evaluate this concept *in vivo*.

Advanced glycation endproducts such as CML and MG-H1 may be more than mere markers of protein damage by MGO. Many studies have shown the importance of the receptor for AGEs (RAGE) in the progression of atherosclerosis.[25,32] In plaques, RAGE is present on macrophages[25] and endothelial cells.[32] Furthermore, it has been demonstrated that extracellular activation of RAGE by AGEs triggers NF-kB signalling.[33] Therefore, the increased AGEs we observed in rupture-prone plaques may be important ligands for RAGE *in vivo*, contributing to a vicious cycle between plaque inflammation and AGE accumulation. However, the data from the current study suggest that the formation of AGEs seem to be a consequence, and not a cause of the pro-inflammatory status, because AGEs did not mediate TNF-induced secretion of inflammatory markers, nor directly induced inflammatory markers. Since we did not find any up-regulation of RAGE in ruptured plaque segments, the

AGE–RAGE interactions may be of lesser importance than intracellular accumulation of AGEs and subsequent cell-death in plaque rupture in human atherosclerosis. These findings are provocative, and deserve further research. In addition, AGEs may contribute to the development of atherosclerosis via the formation of extracellular cross-linking of proteins, as AGE-crosslink breaker ALT-711 attenuates diabetic atherosclerosis in ApoE knock-out mice.[13] Furthermore, induction of oxidative stress by MGO[30] may also contribute to predisposition towards plaque-rupture, as MGO and ROS formation are closely intertwined,[34] and it has been shown that MGO induces apoptosis in an ROS-dependent manner.[35]

Our study has some limitations. First of all, by the cross-sectional design of this study, it is impossible to investigate whether accumulation of AGEs precedes development of rupture-prone lesions. Moreover, in the plaques of the Athero-express study, we defined inflammatory atheroma's as rupture-prone plaques, as these plaques have a similar phenotype as ruptured plaques. We cannot determine in this study if these plaques indeed have the highest risk of plaque rupture, although the finding of higher plaque AGEs in rupture-prone plaques is consistent with the decreased GLO-1 in the ruptured plaques of the CARIM biobank. Furthermore, we cannot exclude residual confounding in the associations between plaque AGEs and plaque phenotype, as data on potential confounders were either not determined in this study (such as Hba1c), or missing in a high proportion of participants (plasma lipids). We found no increase of plaque AGEs in individuals with diabetes. This finding should be interpreted with caution, as we did not measure HbA1c, and 41% of individuals with diabetes used insulin, and 79.5% used oral glucose lowering medication. However, when we adjusted our analyses for insulin and oral glucose lowering medication our results were similar.

Taken together, our study supplies unique data, showing an association between human plaque concentrations of specific MGO-derived AGEs and GLO-1, cell-death, and plaque phenotype. The glycation pathway may be a major player in the progression of stable to rupture-prone plaques and subsequent plaque rupture. Future studies should focus on a causal relationship between AGEs, MGO, and plaque phenotype.

Supplementary material

Supplementary material is available at *European Heart Journal* online.

Funding

This research was performed within the framework of CTMM, the Center for Translational Molecular Medicine (www.ctmm.nl), project PREDICCt (grant 01C-104), and supported by the Dutch Heart Foundation, Dutch Diabetes Research Foundation and Dutch Kidney Foundation. Neither funder had any role in the design, conduct, analysis, or write-up of the research reported. K.W. is supported by the Netherlands Organisation for Scientific Research (NWO-Veni Grant # 91612056) and by a European FP7 Marie Curie grant (FP7-PEOPLE-2012-CIG grant # 322070).

Conflict of interest: none declared.

References

1. Burke AP, Farb A, Malcom GT, Liang YH, Smialek J, Virmani R. Coronary risk factors and plaque morphology in men with coronary disease who died suddenly. *N Engl J Med* 1997;**336**:1276–1282.
2. Farb A, Tang AL, Burke AP, Sessums L, Liang Y, Virmani R. Sudden coronary death. Frequency of active coronary lesions, inactive coronary lesions, and myocardial infarction. *Circulation* 1995;**92**:1701–1709.
3. Virmani R, Burke AP, Farb A, Kolodgie FD. Pathology of the vulnerable plaque. *J Am Coll Cardiol* 2006;**47**(Suppl. 8):C13–C18.
4. Rudd JH, Warburton EA, Fryer TD, Jones HA, Clark JC, Antoun N, Johnstrom P, Davenport AP, Kirkpatrick PJ, Arch BN, Pickard JD, Weissberg PL. Imaging atherosclerotic plaque inflammation with [18F]-fluorodeoxyglucose positron emission tomography. *Circulation* 2002;**105**:2708–2711.
5. Sluimer JC, Gasc JM, van Wanroij JL, Kisters N, Groeneweg M, Sollewijn Gelpke MD, Cleutjens JP, van den Akker LH, Corvol P, Wouters BG, Daemen MJ, Bijnens AP. Hypoxia, hypoxia-inducible transcription factor, and macrophages in human atherosclerotic plaques are correlated with intraplaque angiogenesis. *J Am Coll Cardiol* 2008;**51**:1258–1265.
6. Bonomini F, Tengattini S, Fabiano A, Bianchi R, Rezzani R. Atherosclerosis and oxidative stress. *Histol Histopathol* 2008;**23**:381–390.
7. Basta G, Schmidt AM, De Caterina R. Advanced glycation end products and vascular inflammation: implications for accelerated atherosclerosis in diabetes. *Cardiovasc Res* 2004;**63**:582–592.
8. Kume S, Takeya M, Mori T, Araki N, Suzuki H, Horiuchi S, Kodama T, Miyauchi Y, Takahashi K. Immunohistochemical and ultrastructural detection of advanced glycation end products in atherosclerotic lesions of human aorta with a novel specific monoclonal antibody. *Am J Pathol* 1995;**147**:654–667.
9. Nakamura Y, Horii Y, Nishino T, Shiiki H, Sakaguchi Y, Kagoshima T, Dohi K, Makita Z, Vlassara H, Bucala R. Immunohistochemical localization of advanced glycosylation end products in coronary atheroma and cardiac tissue in diabetes mellitus. *Am J Pathol* 1993;**143**:1649–1656.
10. Schleicher E, Weigert C, Rohrbach H, Nerlich A, Bachmeier B, Friess U. Role of glucoxidation and lipid oxidation in the development of atherosclerosis. *Ann NY Acad Sci* 2005;**1043**:343–354.
11. Schalkwijk CG, Baidoshvili A, Stehouwer CD, van Hinsbergh VW, Niessen HW. Increased accumulation of the glycoxidation product nepsilon-(carboxymethyl)lysine in hearts of diabetic patients: generation and characterisation of a monoclonal anti-CML antibody. *Biochim Biophys Acta* 2004;**1636**:82–89.
12. Goldin A, Beckman JA, Schmidt AM, Creager MA. Advanced glycation end products: sparking the development of diabetic vascular injury. *Circulation* 2006;**114**:597–605.
13. Forbes JM, Yee LT, Thallas V, Lassila M, Candido R, Jandeleit-Dahm KA, Thomas MC, Burns WC, Deemer EK, Thorpe SR, Cooper ME, Allen TJ. Advanced glycation end product interventions reduce diabetes-accelerated atherosclerosis. *Diabetes* 2004;**53**:1813–1823.
14. Watson AM, Soro-Paavonen A, Sheehy K, Li J, Calkin AC, Koitka A, Rajan SN, Brasacchio D, Allen TJ, Cooper ME, Thomas MC, Jandeleit-Dahm KJ. Delayed intervention with AGE inhibitors attenuates the progression of diabetes-accelerated atherosclerosis in diabetic apolipoprotein E knockout mice. *Diabetologia* 2011;**54**:681–689.
15. Brownlee M. Biochemistry and molecular cell biology of diabetic complications. *Nature* 2001;**414**:813–820.
16. Beisswenger PJ, Howell SK, Touchette AD, Lal S, Szwergold BS. Metformin reduces systemic methylglyoxal levels in type 2 diabetes. *Diabetes* 1999;**48**:198–202.
17. Sena CM, Matafome P, Crisostomo J, Rodrigues L, Fernandes R, Pereira P, Seica RM. Methylglyoxal promotes oxidative stress and endothelial dysfunction. *Pharmacol Res* 2012;**65**:497–506.
18. Fukunaga M, Miyata S, Higo S, Hamada Y, Ueyama S, Kasuga M. Methylglyoxal induces apoptosis through oxidative stress-mediated activation of p38 mitogen-activated protein kinase in rat Schwann cells. *Ann NY Acad Sci* 2005;**1043**:151–157.
19. Akhand AA, Hossain K, Mitsui H, Kato M, Miyata T, Inagi R, Du J, Takeda K, Kawamoto Y, Suzuki H, Kurokawa K, Nakashima I. Glyoxal and methylglyoxal trigger distinct signals for map family kinases and caspase activation in human endothelial cells. *Free Radic Biol Med* 2001;**31**:20–30.
20. Ewaschuk JB, Naylor JM, Zello GA. D-lactate in human and ruminant metabolism. *J Nutr* 2005;**135**:1619–1625.
21. Teerlink T, Barto R, Ten Brink HJ, Schalkwijk CG. Measurement of Nepsilon-(carboxymethyl)lysine and Nepsilon-(carboxyethyl)lysine in human plasma protein by stable-isotope-dilution tandem mass spectrometry. *Clin Chem* 2004;**50**:1222–1228.
22. McLellan AC, Thornalley PJ. Glyoxalase activity in human red blood cells fractioned by age. *Mech Ageing Dev* 1989;**48**:63–71.
23. Cudejko C, Wouters K, Fuentes L, Hannou SA, Paquet C, Bantubungi K, Bouchaert E, Vanhoutte J, Fleury S, Remy P, Tailleux A, Chinetti-Gbaguidi G, Dombrowicz D, Staels B, Paumelle R. p16INK4a deficiency promotes IL-4-induced polarization and inhibits proinflammatory signaling in macrophages. *Blood* 2011;**118**:2556–2566.

24. Scheijen JL, Schalkwijk CG. Quantification of glyoxal, methylglyoxal and 3-deoxyglucosone in blood and plasma by ultra performance liquid chromatography tandem mass spectrometry: evaluation of blood specimen. *Clin Chem Lab Med*; doi: 10.1515/cclm-2012-0878. Published online ahead of print 13 March 2013.
25. Cuccurullo C, Iezzi A, Fazia ML, De Cesare D, Di Francesco A, Muraro R, Bei R, Ucchino S, Spigonardo F, Chiarelli F, Schmidt AM, Cuccurullo F, Mezzetti A, Cipollone F. Suppression of RAGE as a basis of simvastatin-dependent plaque stabilization in type 2 diabetes. *Arterioscler Thromb Vasc Biol* 2006;**26**:2716–2723.
26. Nerlich AG, Schleicher ED. N(epsilon)-(carboxymethyl)lysine in atherosclerotic vascular lesions as a marker for local oxidative stress. *Atherosclerosis* 1999;**144**: 41–47.
27. Sakata N, Imanaga Y, Meng J, Tachikawa Y, Takebayashi S, Nagai R, Horiuchi S. Increased advanced glycation end products in atherosclerotic lesions of patients with end-stage renal disease. *Atherosclerosis* 1999;**142**:67–77.
28. Uchida K, Khor OT, Oya T, Osawa T, Yasuda Y, Miyata T. Protein modification by a Maillard reaction intermediate methylglyoxal. immunochemical detection of fluorescent 5-methylimidazolone derivatives in vivo. *FEBS Lett* 1997;**410**: 313–318.
29. Stitt AW, He C, Friedman S, Scher L, Rossi P, Ong L, Founds H, Li YM, Bucala R, Vlassara H. Elevated AGE-modified ApoB in sera of euglycemic, normolipidemic patients with atherosclerosis: relationship to tissue AGEs. *Mol Med* 1997;**3**: 617–627.
30. Brouwers O, Niessen PM, Ferreira I, Miyata T, Scheffer PG, Teerlink T, Schrauwen P, Brownlee M, Stehouwer CD, Schalkwijk CG. Overexpression of glyoxalase-I reduces hyperglycemia-induced levels of advanced glycation end products and oxidative stress in diabetic rats. *J Biol Chem* 2011; **286**:1374–1380.
31. Li L, Sawamura T, Renier G. Glucose enhances human macrophage LOX-1 expression: role for LOX-1 in glucose-induced macrophage foam cell formation. *Circ Res* 2004;**94**:892–901.
32. Harja E, Bu DX, Hudson BI, Chang JS, Shen X, Hallam K, Kalea AZ, Lu Y, Rosario RH, Oruganti S, Nikolla Z, Belov D, Lalla E, Ramasamy R, Yan SF, Schmidt AM. Vascular and inflammatory stresses mediate atherosclerosis via RAGE and its ligands in apoE-/- mice. *J Clin Invest* 2008;**118**:183–194.
33. Bierhaus A, Schiekofer S, Schwaninger M, Andrassy M, Humpert PM, Chen J, Hong M, Luther T, Henle T, Kloting I, Morcos M, Hofmann M, Tritschler H, Weigle B, Kasper M, Smith M, Perry G, Schmidt AM, Stern DM, Haring HU, Schleicher E, Nawroth PP. Diabetes-associated sustained activation of the transcription factor nuclear factor-kappaB. *Diabetes* 2001;**50**:2792–2808.
34. Paneni F, Mocharla P, Akhmedov A, Costantino S, Osto E, Volpe M, Luscher TF, Cosentino F. Gene silencing of the mitochondrial adaptor p66(Shc) suppresses vascular hyperglycemic memory in diabetes. *Circ Res* 2012;**111**:278–289.
35. Amicarelli F, Colafarina S, Cattani F, Cimini A, Di Ilio C, Ceru MP, Miranda M. Scavenging system efficiency is crucial for cell resistance to ROS-mediated methylglyoxal injury. *Free Rad Biol Med* 2003;**35**:856–871.